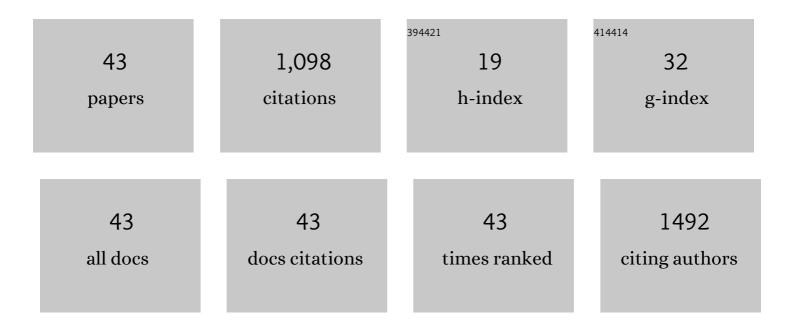
## Jianjun Liao

List of Publications by Year in descending order

Source: https://exaly.com/author-pdf/4072390/publications.pdf Version: 2024-02-01



#	Article	IF	CITATIONS
1	Constructing a 3D interconnected "trap-zap―β-CDPs/Fe-g-C3N4 catalyst for efficient sulfamethoxazole degradation via peroxymonosulfate activation: Performance, mechanism, intermediates and toxicity. Chemosphere, 2022, 294, 133780.	8.2	14
2	Toward efficient electrocatalytic oxygen evolution with a low concentration baking soda activated IrO <sub><i>x</i></sub> surface in a hydrothermal medium. Materials Chemistry Frontiers, 2022, 6, 1282-1291.	5.9	2
3	Amorphous–Amorphous Coupling Enhancing the Oxygen Evolution Reaction Activity and Stability of the NiFe-Based Catalyst. ACS Applied Materials & Interfaces, 2022, 14, 15205-15213.	8.0	16
4	Laser-Induced Graphene-Based Wearable Epidermal Ion-Selective Sensors for Noninvasive Multiplexed Sweat Analysis. Biosensors, 2022, 12, 397.	4.7	18
5	Enriched nitrogen-doped carbon derived from expired drug with dual active sites as effective peroxymonosulfate activator: Ultra-fast sulfamethoxazole degradation and mechanism insight. Chemical Engineering Journal, 2022, 446, 137407.	12.7	18
6	Competitive smartphone-based portable electrochemical aptasensor system based on an MXene/cDNA-MB probe for the determination of Microcystin-LR. Sensors and Actuators B: Chemical, 2022, 369, 132164.	7.8	14
7	Surface Engineering and Builtâ€In Electric Field within Copper Sulfide/Graphitic Carbon Nitride Photocatalyst for Extremely Enhanced Charge Separation and Broadâ€Spectrum Pharmaceuticals and Personal Care Products Degradation. Solar Rrl, 2021, 5, .	5.8	11
8	<i>In situ</i> formation of grain boundaries on a supported hybrid to boost water oxidation activity of iridium oxide. Nanoscale, 2021, 13, 13845-13857.	5.6	6
9	Ag and Fe <sub>3</sub> O <sub>4</sub> Comodified WO <sub>3–Â<i>x</i></sub> Nanocomposites for Catalytic Photothermal Degradation of Pharmaceuticals and Personal Care Products. ACS Applied Nano Materials, 2021, 4, 1898-1905.	5.0	14
10	Super-structural 2D ultrathin carbon nitride/acrylate boron silane polymer with multi-function for enhancing antifouling performance. Journal of Coatings Technology Research, 2021, 18, 1051-1064.	2.5	1
11	Zinc sulfide quantum dots/zinc oxide nanospheres/bismuth-enriched bismuth oxyiodides as Z-scheme/type-II tandem heterojunctions for an efficient charge separation and boost solar-driven photocatalytic performance. Journal of Colloid and Interface Science, 2021, 592, 259-270.	9.4	35
12	Analysis of imidacloprid residues in mango, cowpea and water samples based on portable molecular imprinting sensors. PLoS ONE, 2021, 16, e0257042.	2.5	11
13	A synergistic promotion strategy for selective trapping and sensing of lead(II) by oxygen-vacancy and surface modulation of MnO2 nanoflowers. Sensors and Actuators B: Chemical, 2021, 345, 130384.	7.8	10
14	Highly sensitive and selective H2O2 sensors based on ZnO TFT using PBNCs/Pt-NPs/TNTAs as gate electrode. Sensors and Actuators B: Chemical, 2021, 349, 130791.	7.8	13
15	Smartphone-based molecularly imprinted sensors for rapid detection of thiamethoxam residues and applications. PLoS ONE, 2021, 16, e0258508.	2.5	5
16	IrO <sub>x</sub> Nanoclusters Modified by BaCO <sub>3</sub> Enable ″Two Birds with One Stone″ in Solar-Driven Direct Unbuffered Seawater Electrolysis. ACS Applied Materials & Interfaces, 2021, 13, 61088-61097.	8.0	10
17	Wireless water quality monitoring and spatial mapping with disposable whole-copper electrochemical sensors and a smartphone. Sensors and Actuators B: Chemical, 2020, 306, 127557.	7.8	42
18	Cerium Surface-Engineered Iridium Oxides for Enhanced Oxygen Evolution Reaction Activity and Stability. ACS Applied Energy Materials, 2020, 3, 4432-4440.	5.1	17

Jianjun Liao

#	Article	IF	CITATIONS
19	An amorphous lanthanum–iridium solid solution with an open structure for efficient water splitting. Journal of Materials Chemistry A, 2020, 8, 12518-12525.	10.3	24
20	Cost-effective, wireless, and portable smartphone-based electrochemical system for on-site monitoring and spatial mapping of the nitrite contamination in water. Sensors and Actuators B: Chemical, 2020, 319, 128221.	7.8	57
21	Assembly of a Highly Active Iridium-Based Oxide Oxygen Evolution Reaction Catalyst by Using Metal–Organic Framework Self-Dissolution. ACS Applied Materials & Interfaces, 2020, 12, 29414-29423.	8.0	6
22	Theoretical and experimental insights into the electrochemical heavy metal ionÂsensing with nonconductive nanomaterials. Current Opinion in Electrochemistry, 2019, 17, 1-6.	4.8	6
23	A real-time on-line photoelectrochemical sensor toward chemical oxygen demand determination based on field-effect transistor using an extended gate with 3D TiO2 nanotube arrays. Sensors and Actuators B: Chemical, 2019, 289, 106-113.	7.8	44
24	Functional Sensing Interfaces of PEDOT:PSS Organic Electrochemical Transistors for Chemical and Biological Sensors: A Mini Review. Sensors, 2019, 19, 218.	3.8	48
25	Electrochemical and density functional theory investigation on the differential behaviors of core-ring structured NiCo 2 O 4 nanoplatelets toward heavy metal ions. Analytica Chimica Acta, 2018, 1022, 37-44.	5.4	39
26	The crystal facet-dependent electrochemical performance of TiO2 nanocrystals for heavy metal detection: Theoretical prediction and experimental proof. Sensors and Actuators B: Chemical, 2018, 271, 195-202.	7.8	31
27	First-principles investigation of metal-doped cubic BaTiO 3. Materials Research Bulletin, 2017, 96, 372-378.	5.2	39
28	Regulation of the Electroanalytical Performance of Ultrathin Titanium Dioxide Nanosheets toward Lead Ions by Non-Metal Doping. Nanomaterials, 2017, 7, 327.	4.1	14
29	A miniature photoelectrochemical sensor based on organic electrochemical transistor for sensitive determination of chemical oxygen demand in wastewaters. Water Research, 2016, 94, 296-304.	11.3	32
30	Enhanced photoelectrochemical performance of quantum dot-sensitized TiO <sub>2</sub> nanotube arrays with Al <sub>2</sub> O <sub>3</sub> overcoating by atomic layer deposition. Physical Chemistry Chemical Physics, 2016, 18, 17404-17413.	2.8	44
31	Electrochemically self-doped hierarchical TiO <sub>2</sub> nanotube arrays for enhanced visible-light photoelectrochemical performance: an experimental and computational study. RSC Advances, 2016, 6, 46871-46878.	3.6	20
32	Improving photoelectrochemical performance on quantum dots co-sensitized TiO2 nanotube arrays using ZnO energy barrier by atomic layer deposition. Applied Surface Science, 2016, 388, 352-358.	6.1	19
33	Synthesis and Characterization of Hierarchical Structured TiO2Nanotubes and Their Photocatalytic Performance on Methyl Orange. Journal of Nanomaterials, 2015, 2015, 1-8.	2.7	1
34	Highly selective and sensitive glucose sensors based on organic electrochemical transistors using TiO2 nanotube arrays-based gate electrodes. Sensors and Actuators B: Chemical, 2015, 208, 457-463.	7.8	69
35	Organic electrochemical transistor based biosensor for detecting marine diatoms in seawater medium. Sensors and Actuators B: Chemical, 2014, 203, 677-682.	7.8	20
36	Uniform deposition of water-soluble CdS quantum dots on TiO2 nanotube arrays by cyclic voltammetric electrodeposition: Effectively prevent aggregation and enhance visible-light photocatalytic activity. Electrochimica Acta, 2013, 108, 296-303.	5.2	33

Jianjun Liao

#	Article	IF	CITATIONS
37	Effects of Surface Modification of Nanotube Arrays on the Performance of CdS Quantum-Dot-Sensitized Solar Cells. International Journal of Photoenergy, 2013, 2013, 1-10.	2.5	6
38	Nitrogen-Doped TiO <sub><b>2</b></sub> Nanotube Arrays with Enhanced Photoelectrochemical Property. International Journal of Photoenergy, 2012, 2012, 1-7.	2.5	21
39	Free-standing open-ended TiO2 nanotube membranes and their promising through-hole applications. Chemical Engineering Journal, 2012, 211-212, 343-352.	12.7	28
40	Hierarchical structured TiO2 nano-tubes for formaldehyde sensing. Ceramics International, 2012, 38, 6341-6347.	4.8	57
41	Photocatalytic Degradation of Methyl Orange Using a TiO <sub>2</sub> /Ti Mesh Electrode with 3D Nanotube Arrays. ACS Applied Materials & Interfaces, 2012, 4, 171-177.	8.0	138
42	Fabrication of freeâ€standing TiO <sub>2</sub> nanotube membranes with throughâ€hole morphology. Crystal Research and Technology, 2012, 47, 731-737.	1.3	6
43	Fabrication and photocatalytic properties of free-standing TiO2 nanotube membranes with through-hole morphology. Materials Characterization, 2012, 66, 24-29.	4.4	39